JOURNAL OF PHYSICAL ORGANIC CHEMISTRY
J. Phys. Org. Chem. 2002; **15:** 385–391
Published online in Wiley InterScience (www.interscience.wiley.com). DOI: 10.1002/poc.515

4-Alkylbenzopyrylium perchlorates as C—H Acidic compounds

U.-W. Grummt[1]* and P. Czerney[2]

[1]Institut für Physikalische Chemie der Friedrich-Schiller Universität Jena, Lessingstrasse 10, D-07743 Jena, Germany
[2]Dyomics GmbH, Winzerlaer Strasse 2A, D-07743 Jena, Germany

Received 4 December 2001; revised 20 February 2002; accepted 18 March 2002

ABSTRACT: 7-Alkyl-5,6-dihydro-3-methoxy(naphtho[1,2*b*]-1-benzopyrylium) compounds are acidochromic due to CH acidity of the 7-alkyl substituent. Their acidity exponents are $4 < pK_a < 5$ and $1 < pK_a < 3$ regardless of whether the carbocation generated by deprotonation is resonance stabilized by a phenyl substituent or not. The thermodynamic equilibrium data were obtained via UV–vis spectroscopy. The activation parameters for protonation and deprotonation reactions were derived from rapid mixing experiments. *Ab initio* calculations with model compounds are presented in order to rationalize the experimental findings. The title compounds are useful objects to study the kinetics of proton-transfer kinetics to and from carbon. Copyright © 2002 John Wiley & Sons, Ltd.

KEYWORDS: 4-alkylbenzopyrylium perchlorates; C—H acidity; protonation kinetics

INTRODUCTION

Functional dyes have attracted interest as active materials for optochemical sensing,[1] particularly in the field of bioscience. The benzopyrylium heterocycle is a very useful structural unit for the synthesis of a vast variety of functional dyes.[2,3] In the course of our investigations on pyrylium dyes we have recently discovered that certain substituted 7-alkylbenzopyrylium compounds exhibit reversible acidochromism in the visible spectral range due to CH protonation and deprotonation. Proton-transfer reactions involving carbon have up until now been studied mostly with photogenerated enols, phenol tautomers and related compounds.[4] When tautomerization processes occur, several kinetically indistinguishable mechanisms may co-exist, thus significantly complicating kinetic investigations since the protonation and deprotonation sites occur within the same molecule. This situation is, however, somewhat simplified in the case of the 4-alkylpyrylium compounds depicted in Scheme 1 which are in equilibrium with their 4-methylenepyran counterparts.

Since the Gibbs free energy difference between the protonated and the unprotonated molecules is comparatively small, the equilibrium can be shifted to either side by varying the pH of the solution. With the help of rapid mixing techniques kinetic studies can be performed on these systems. With a proper substituent choice (R), the relative thermodynamic stabilities of both forms can be easily controlled. Scheme 2 contains an overview of the compounds selected for these investigations.

**Correspondence to:* U.-W. Grummt, Institut für Physikalische Chemie der Friedrich-Schiller Universität Jena, Lessingstrasse 10, D-07743 Jena, Germany.
E-mail: cug@uni-jena.de

EXPERIMENTAL

Synthesis and materials

The synthesis of the dyes **3, 4** and **5** has been described.[5] Compounds **1** and **2** were similarly prepared according to the following procedure.

To a solution of 1.25 mmol of the corresponding 7*H*-(1*H*-benzotriazol-1-yl)-5,6-dihydronaphtho[1,2*b*]benzopyran[6] in 30 ml of dry tetrahydrofuran (THF) under nitrogen at −78 °C was added 1.25 mmol (0.62 ml, 2 M in pentane) of *n*-BuLi. The blue solution was stirred at −78 °C for 30 min before adding 1.25 mmol of (bromomethyl)benzene in 20 ml of dry THF. The mixture was stirred and allowed to warm to room temperature overnight. After adding 40 ml of a saturated aqueous NH_4Cl solution, the mixture was extracted twice with 30 ml of diethyl ether. The combined extracts were then washed with water and dried with $MgSO_4$. The solvent was removed *in vacuo* and 30 ml of glacial acetic acid were added to the resulting oil. After the addition of 3 ml of aqueous $HClO_4$ (70%) and 50 ml of water, the benzopyrylium salts precipitated. The products were recrystallized from acetic acid.

In order to isolate the neutral dye bases, the oily residue was dissolved in acetic acid and then diluted with water or aqueous ammonia solution until precipitation

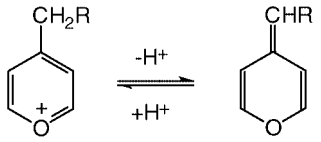

Scheme 1

occurred. The neutral dyes were recrystallized from nitromethane or acetonitrile and purified by column chromatography with basic alumina.

*5,6-Dihydro-3-methoxy-7-methylidenebenzyl-(naphtho[1,2b]-1-chromene) (the conjugate neutral base of **1**).* Yield 260 mg (60%); $C_{25}H_{20}O_2 \cdot H_2O$; $M_r = 352.43$ g mol^{-1}; m.p. = 138–142 °C. Analysis: calc. C 81.06, H 5.99; found C 80.98, H 5.73%. ^{1}H NMR (250 MHz, $CDCl_3$): δ 2.63 (t, $J = 7.6$ Hz, 2H), 2.89 (t, $J = 7.4$ Hz, 2H), 3.79 (s, 3H), 6.38 (s, 1H), 6.81–6.89 (m, 3H), 7.19–7.30 (m, 8H), 7.62 (d, $J = 9.1$ Hz, 1H). ^{13}C NMR (62.0 MHz, DMSO-d_6): δ 22.4, 27.1, 55.2, 111.5, 111.8, 113.2, 114.9, 117.3, 120.3, 121.7, 122.6, 122.9, 126.4, 127.3, 127.4, 128.3, 128.4, 129.3, 138.2, 138.4, 143.7, 151.5, 159.5. MS (70 eV): *m/z* (%) 352 [M^+] (100), 315 (80).

*7-(2,6-Dichlorobenzyl)-5,6-dihydro-3-methoxy-(naphtho[1,2b]-1-benzopyrylium)perchlorate (**2**).* Yield 150 mg (23%); $C_{25}H_{19}Cl_3O_6$; $M_r = 521.78$ g mol^{-1}; m.p. = 254–262 °C. Analysis: calc. C 57.55, H 3.67, Cl 20.36; found C 57.43, H 3.92, Cl 19.37%. ^{1}H NMR (250 MHz, $CDCl_3$–CF_3CO_2D): δ 3.17 (s, 4H), 3.99 (s, 3H), 4.99 (s, 2H), 6.92 (d, $J = 2.4$ Hz, 1H), 7.10 (dd, $J = 2.4$, 9.0 Hz, 1H), 7.21–7.28 (m, 1H), 7.32–7.38 (m 2H), 7.66–7.74 (m, 1H), 7.87–8.11 (m, 3H), 8.40 (d, $J = 9.0$ Hz, 1H). ^{13}C NMR (62.0 MHz, $CDCl_3$–CF_3CO_2D): δ 24.3, 26.7, 33.0, 56.5, 114.1, 116.7, 118.1, 119.3, 123.7, 126.1, 128.6, 129.3, 129.4, 130.1, 132.2, 132.9, 135.5, 136.8, 149.3, 153.3, 163.6, 169.1, 169.4.

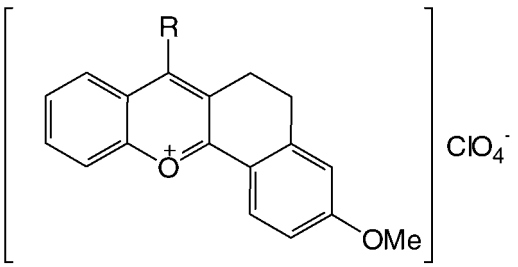

	R
1	-CH_2-C_6H_5
2	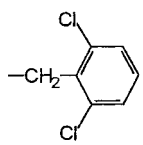
3	-$(CH_2)_2$-C_6H_5
4	-$(CH_2)_3$-C_6H_5
5	-$(CH_2)_3$-CH_2Cl

Scheme 2

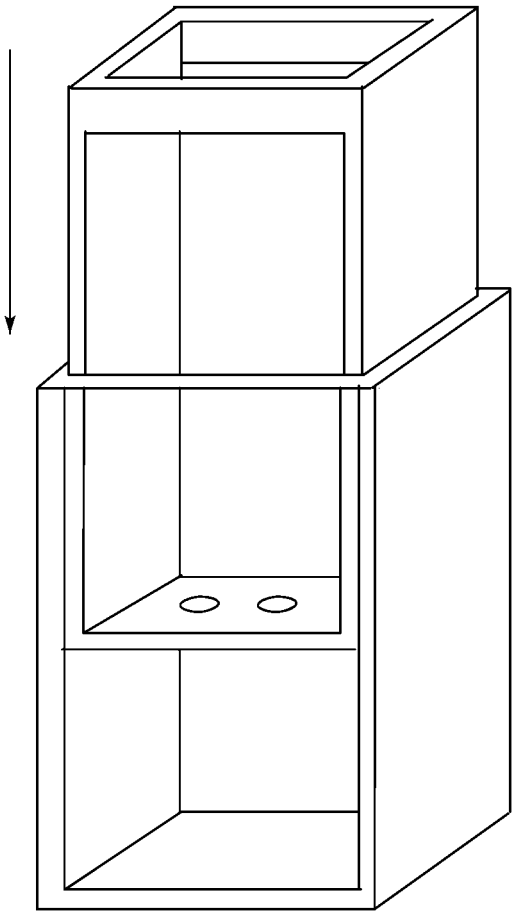

Figure 1. Sketch of the mixing cell used for the kinetic UV–vis spectroscopic measurements

Instrumentation and methods

^{1}H and ^{13}C NMR spectra were recorded with Bruker DRX 400 and AC 250 spectrometers, respectively. Mass spectra were measured with a Finnigan Mat SSQ710 mass spectrometer. Stationary UV–vis absorption spectra were recorded with a Perkin-Elmer Lambda 19 UV/VIS–NIR spectrometer. Kinetic measurements were performed with a Specord S 100 diode-array spectrometer (Analytik Jena) equipped with a simple laboratory-made cell (Fig. 1) to ensure rapid mixing within a few tenths of a second. The cell was inserted in a water thermostat. The normal absorption cell was filled to half height with one

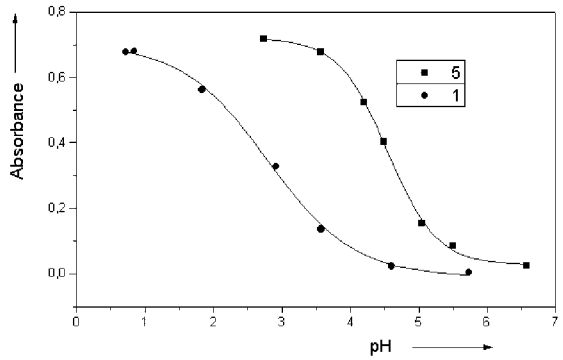

Figure 2. Titration curve for salt **1**, at [**1**] = 4.9×10^{-5} mol l^{-1} in 2-propanol–water, $\lambda_{rec} = 456$ nm, and titration curve of salt **5** at [**5**] = 4.9×10^{-5} mol l^{-1} in 2-propanol–water; $\lambda_{rec} = 450$ nm; T = 298 K for both records

of the solutions, then the 'piston' was inserted until it touched the liquid surface. After reaching thermal equlibrium, the other solution kept at the correct temperature was cautiously filled in. Mixing and triggering of the spectrometer were performed manually by pushing the piston rapidly down.

A 1:1 (v/v) mixture of water and 2-propanol was used as the solvent for all spectroscopic and kinetic measurements. Aqueous citrate–phosphate buffers[7] were used for the range $2.23 < \text{pH} < 8$ and aqueous hydrochloric acid–potassium chloride buffers for $1.2 < \text{pH}\ 2.2$.[7]

In the case of **1** and **2**, the pH of the dye solutions was adjusted before mixing with the smallest possible amount of aqueous sodium hydroxide solution necessary to obtain a vanishing pyrylium salt absorption. Dilute aqueous perchloric acid in the same solvent mixture was used as the other component for mixing. For all other substances, the kinetics were monitored in the opposite direction: The dye solution was acidified until the equilibrium was shifted nearly quantitatively to the pyrylium form and buffer solutions were used for mixing.

With the exception of solutions of **1** and **2**, where the

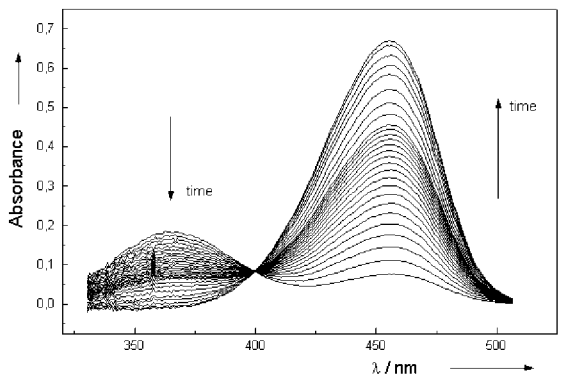

Figure 3. Reaction spectra of **1** recorded at 298 K; time interval 0.7 s. An increasing number of spectra have been omitted for clarity towards the end of the reaction. Solution 1, [**1**] = 9.9×10^{-5} mol l^{-1}; solution 2, + 1.75 ml of 70% aqueous $HClO_4$ in 100 ml of solvent mixture

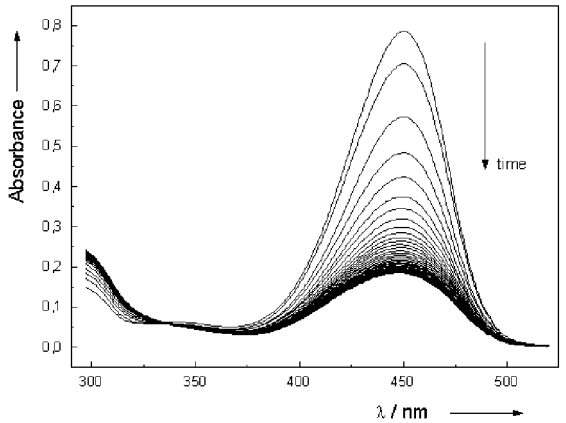

Figure 4. Reaction spectra of **5** recorded at 298 K; time interval 2.0 s. Solution 1, [**5**] = 1.2×10^{-4} mol l^{-1}; solution 2, at pH 5.0 (buffer)

pH was adjusted to pH < 1, the ionic strength of the solutions was kept below 0.1 M. The effect of the ionic strength on the acidochromic equilibria was negligibly small under these conditions. In order to quantify the effect of a variation of the ionic strength, we recorded several series of absorption spectra as a function of KCl concentration up to 0.5 M. Below 0.1 M the variation of the absorbance was within 3%, which is the range of the overall reproducibility of the absorbance measurement including sample preparation. Significant salt effects are observable at an ionic strength above 0.1 M in the region of $\text{pH} \approx \text{p}K_a$. All pH measurements were performed using an Hl 9318 pH meter (Hanna Instruments) with temperature correction and a glass electrode.

Principal component analyses[8] were performed with the raw absorbance data without any preprocessing using a laboratory-written program. A modified version of Schuetz *et al.*'s ALAU[9] was used for all non-linear data fitting. Hartree–Fock quantum chemical calculations were performed with the Gaussian 98 package[10] on a LINUX PC employing the 6–31 + G(d) basis set. Frequency calculations were performed in order to obtain the thermodynamic functions and to validate the stationary points found as energetic minima.

Solvent effects were estimated using Onsager's reaction field model.[11] More sophisticated solvent cage models could not be applied because of occasional convergence problems and the high computational demand.

RESULTS AND DISCUSSION

Spectroscopic and kinetic experiments

The acidochromism observed in these systems is demonstrated by two examples of titration curves and

Table 1. Acidity exponents and thermodynamic and kinetic parameters of the pyrylium perchlorates **1**–**5**

Compound	pK_a (298 K)	$\Delta G^{\ominus}$ (kJ mol^{-1})	$\Delta H^{\ominus}$ (kJ mol^{-1})	$\Delta S^{\ominus}$ (J mol^{-1} K^{-1})	$\Delta H^{\neq}$ (kJ mol^{-1})	$\Delta S^{\neq}$ (J mol^{-1}K^{-1})
1	2.90 ± 0.09	16.5 ± 0.5	10.2 ± 0.7	-21.7 ± 2.2	54.3 ± 4.9	-62.9 ± 5.2
2	1.39 ± 0.16	7.9 ± 0.9	7.95 ± 1.10	—	59.7 ± 1.4	-60.0 ± 1.4
3	4.50 ± 0.10	25.7 ± 0.6	18.5 ± 0.7	-24.1 ± 2.1	47.8 ± 1.5	—
4	4.62 ± 0.05	26.5 ± 0.3	21.8 ± 1.9	-15.9 ± 6	58.2 ± 7.3	—
5	4.55 ± 0.03	26.0 ± 0.2	18.2 ± 0.6	-26.1 ± 1.8	56.8 ± 7.2	—

the results of the rapid mixing experiments shown in Figs 2–4.

The pK_a values (at 20 °C) of the compounds studied are given in Table 1. They were obtained from directly fitting the absorbance A at the absorption maxima to the function

$$A(\mathrm{pH}) = \frac{A_D 10^{\mathrm{pH}-pK_a} + A_{DH^+}}{1 + 10^{\mathrm{pH}-pK_a}}$$

where A_D and A_{DH^+} are the absorbances of the pure species. Standard reaction enthalpies, $\Delta_R H^{\ominus}$, and entropies, $\Delta_R S^{\ominus}$, derived from linear regressions using

$$\ln K_a = -\frac{\Delta_R H^{\ominus}}{R}\frac{1}{T} + \frac{\Delta_R S^{\ominus}}{R}$$

are also given in Table 1 together with the activation data.

The stabilizing effect of the 4-benzyl substituent on the neutral colorless form is obvious from the thermodynamic data. Owing to the stronger electron-withdrawing 2,6-dichlorophenyl ring, cation **2** is a significantly stronger acid than **1**. The entropy changes are negative throughout. Upon dissociation, the largely delocalized positive charge on the pyrylium dye is transferred to the small hydronium ion which is more strongly solvated. In addition, low-frequency vibrational modes of the pyrylium cation vanish which contribute to the negative entropy change. Owing to large scatter of the the equilibrium data for species **2**, a meaningful entropy change could not be obtained. From a casual inspection of Figs 3 and 4 one might assume a simple acid–base equilibrium with only one linearly independent reaction. However, principal component analyses of all sets of absorption spectra obtained from the rapid mixing experiments clearly yielded two components, as can be seen from the abstract eigenspectra, cf. Figs 5 and 6 for dyes **1** and **5**, respectively. The largest eigenvalues generally contain 94–96% of the total data variance whereas two eigenvalues describe 99.99%. The neglected variance is distributed over many insignificant eigenvalues.

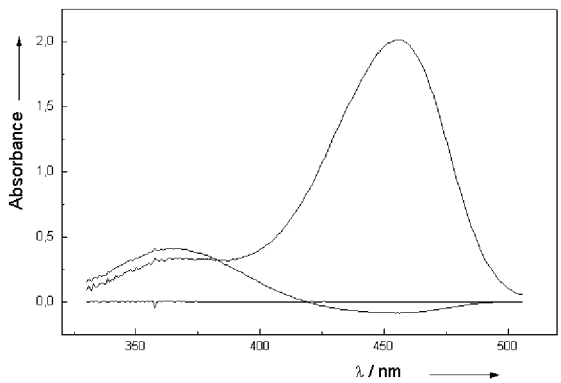

Figure 5. Principal component analysis of the set shown in Fig. 3 (compound **1**): first three abstract eigenspectra

We therefore fitted the kinetics to a sum of two exponentials. It is well known that pyrylium salts of this type are prone to a nucleophilic attack at the C-2 ring position by the hydroxide ion followed by ring opening in stronger alkaline solution[12,13] (cf. Scheme 3). The *trans* chalcone form has been isolated and characterized, for instance, in the case of a pyrylium salt unsubstituted in the 4-position.[14] For the compounds studied here the solvolysis reaction is reversible and gives rise to the second pseudo-first-order process as a consecutive reaction. Short-lived intermediates cannot be detected in the time resolution of our experiments.

Assuming that these bimolecular reactions obey a pseudo-first-order rate law, the solution of the set of differential equations $\Theta_{1,2}$ describing the mechanism given in Scheme 3 is as follows:[15]

$$\Theta_{1,2} = \frac{k_H + k_{-H} + k_{open} + k_{close}}{2}$$

$$\pm\sqrt{\left(\frac{k_H - k_{-H} + k_{open} + k_{close}}{2}\right)^2 + k_{-H}(k_H - k_{close})}$$

This equation simplifies to

$$\Theta_1 = k_H + k_{-H} \quad \text{and} \quad \Theta_2 = k_{open} + k_{close}$$

assuming that the first equilibrium is established significantly faster than the second, which is clearly the case for the compounds studied here since the Θ_1 values are at least two orders of magnitude larger than Θ_2. We evaluated only Θ_1 further, which can additionally justified by the fact that the second equilibrium contributes only about 5% to the total variance of the

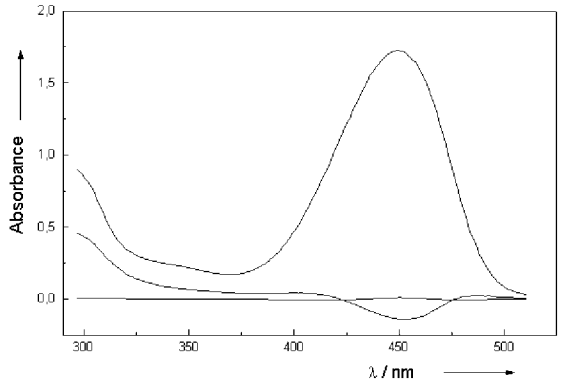

Figure 6. Principal component analysis of the set shown in Fig. 4 (compound **5**): first three abstract eigenspectra

kinetic data. The reciprocal lifetimes $\Theta_{1,2}$ obtained from the fitting procedure may be interpreted as being rate constants for a particular reaction step only in the case of consecutive reactions without reversible steps and branching. For a reversible step, the exponential is the sum of the forward and the reverse reaction as shown above. If, however, the kinetics of the reaction are measured far from the equilibrium point then the rate constant of the reverse reaction can be neglected, conditions which are fulfilled in these experiments. We could show that the observed exponentials were strictly proportional to the final hydronium ion concentration in the mixing experiments (perchloric acid concentration) for compounds **1** and **2** and also further compounds of the same structural type not included here (the solution concentrations ranged from 0.005 to 0.06 M). We also confirmed a pseudo reaction order for the reverse reaction with compound **5**. The rate constants are invariant with respect to the recording wavelength in all cases. Equating of the first exponentials in the biexponential fits as (pseudo) first-order rate constants for the protonation and deprotonation of the compounds studied here is therefore justified.

For the protonation reaction we may safely assume that the hydronium ion is the only protonating species. However, the mechanism of the deprotonation could be more complex because buffer anions may contribute to the rate. This means that the kinetic data for deprotonation refer to the overall reaction. Decomposition into individual contributions from the hydroxide ion and the buffer anions needs further investigation.

The activation enthalpies for the deprotonation of compounds **1** and **2** (ca 65 kJ mol^{-1}) are larger than those of **3–5**. (Note that $\Delta H^{\neq}$ given in Table 1 refers to the protonation reaction.)

For these compounds it is probably justified to use the bimolecular rate constant determined as

$$k_{H^+} = k_{obs} \times 10^{pH}$$

to calculate the activation entropies from the Arrhenius pre-exponential factor A using Eyring's relation:

$$\Delta_R S^{\neq} = R \ln A \frac{h}{e k_B T}$$

For compounds **1** and **2** we obtain $\Delta S^{\neq} = -63 \pm 5$ and -60 ± 1 J mol^{-1} K^{-1}, respectively, for the protonation reaction.

Quantum chemical calculations

HF/6–31 + G(d) calculations were performed on the model cations 4-methylpyrylium, 2-methoxy-4-methylpyrylium, 3-methoxy-4-methylpyrylium and 4-benzylpyrylium. Ammonia was used as the proton-accepting base instead of the much stronger base HO^- or the weaker base water since we were unable to find stationary points for the van der Waals complexes of 4-alkylpyrylium and the hydroxide ion, 4-methylenepyran and water, 4-methylpyrylium and water and 4-methylenepyran and hydronium. The geometries of both van der Waals complexes and the transition structures were fully optimized and the nature of the stationary point was characterized via frequency calculations. The aim of the calculations was to predict the effect of donor substituents in the 2- or 3-position on the thermodynamics and kinetics of the protonation/deprotonation reactions and to rationalize the higher activation barriers of the 4-benzylpyrylium dyes with respect to the 4-alkyl compounds. Since the reaction coordinate is essentially determined by the heavy atom motion, proton tunnelling was not considered.

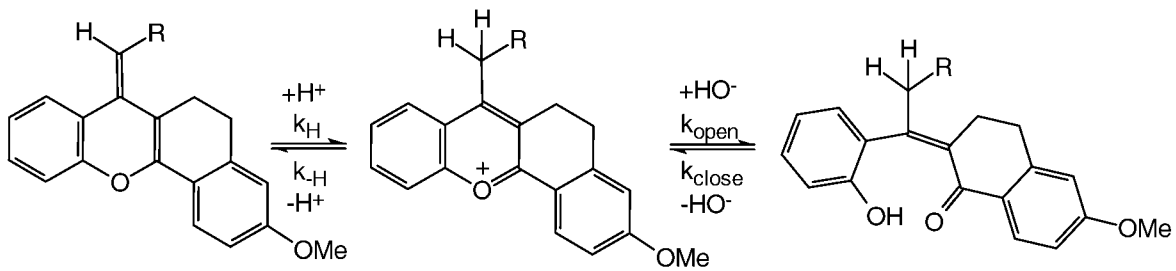

Scheme 3

Table 2. Calculated thermodynamic data for the proton-transfer equilibria between 4-methylpyrylium cations and ammonia, and for the transition states; the top three rows refer to gas-phase and the bottom three rows to solvent calculations; units are kJ mol^{-1} for ΔH and ΔG and J mol^{-1} K^{-1} for ΔS

	4-Methylpyrylium		3-Methoxy-4-methylpyrylium		2-Methoxy-4-methylpyrylium		4-Benzylpyrylium	
Parameter	Transition state	4-Methylenepyran	Transition state	4-Methylenepyran	Transition state	4-Methylenepyran	Transition state	4-Methylenepyran
ΔH	97.5	89.2	100.5	90.0	131.0	129.8	106.3	84.6
ΔG	110.9	97.5	114.7	94.2	147.8	139.4	114.7	90.4
ΔS	−50.6	−28.0	−47.7	−13.8	−56.1	−32.2	−28.0	−19.7
ΔH	89.2	69.5	95.4	67.8	120.6	106.3	105.1	71.2
ΔG	111.8	75.8	109.3	78.2	122.2	97.5	113.9	84.6
ΔS	−22.3	−20.9	−46.5	−35.2	−5.4	29.3	−29.3	−44.8

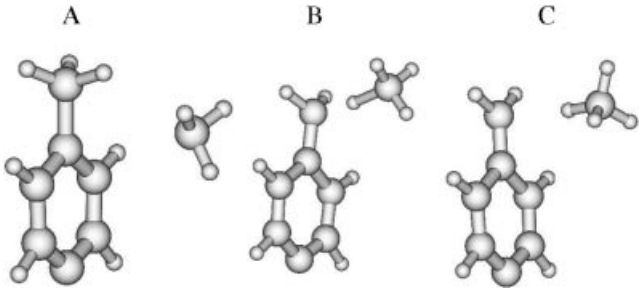

Figure 7. Geometries of the van der Waals complex of 4-methylpyrylium with ammonia (A), the transition structure (B) and the van der Waals complex of 4-methylenepyran with ammonium (C)

Table 2 shows the results where the top three rows of data are gas-phase results and the bottom three rows refer to Onsager's reaction field ($\epsilon_r = 21$). All data are given relative to the pyrylium cation–ammonia complex.

Although the calculatuions were performed on model compounds and the base differs from experiment and, in the case of solvent calculations, a primitive model was used, the experimental trends are well reproduced in the calculations. The thermodynamically more stable form for all model compounds is the pyrylium salt. The transition structure lies close to the product (4-methylenepyran–ammonium complex) as demonstrated in Fig. 7. The reaction and activation entropies are negative (with one exception, which needs further consideration). Methoxy substitution in the 2-position stabilizes the pyrylium salt and increases the activation enthalpy for deprotonation. This is in accord with chemical intuition. Note that the compounds are phenylogous 2-methoxypyrylium salts. Methoxy substitution in the 3-position is predicted to have a negligible effect. The 4-benzylpyrylium salts exhibit a larger activation enthalpy than the 4-alkylpyrylium salts. This is in full accord with the experimental findings. The equilibrium data predicted differ insignificantly.

CONCLUSIONS

7-Alkyl-5,6-dihydro-3-methoxy(naphtho[1,2*b*]-1-benzopyrylium) perchlorates are C—H acidic with acidity exponents that can be tuned over a wide range. The benzopyrylium cation resulting from alkyl = benzyl is a moderately strong acid due to resonance stabilization of the conjugate neutral base ($2 < pK_a < 3$). Electron-withdrawing substituents at the phenyl group further enhance the acidity. Saturated alkyl substituents lead to weak acids ($5 < pK_a < 6$). The pK_a regions may be extended to an even wider span by further structure variations. Owing to the considerable activation enthalpies of about 45–65 kJ mol^{-1}, the protonation or deprotonation reaction is easily kinetically monitored in the range of tenths of seconds to minutes.

Ab initio calculations on 4-alkylpyrylium cations and 4-methylenepyran at the HF/6–31 + G* level are useful in explaining the essential thermodynamic and kinetic substituent effects. In particular, donor substituents in the 2-position stabilize the pyrylium salt and increase the activation enthalpy for deprotonation, which is fully in accord with experiment. The title compounds are useful objects to study the kinetics of proton-transfer kinetics from and to carbon. They deserve further more detailed investigations.

Acknowledgements

Preliminary stopped-flow experiments were performed by Dr Wannowius, TU Darmstadt, which is gratefully acknowledged. We thank Dr Jesser for the synthesis of compounds **1** and **2**.[16]

REFERENCES

1. Wolfbeis OS, Boisde G. In *Sensors–A Comprehensive Survey*, vol. 3, Göpel W, Hesse J, Zemels JN (eds). VCH: Weinheim, 1992; 867–930.
2. Czerney P, Grummt U-W, Günther W. *J. Prakt. Chem.* 1998; **340**: 214–222.
3. (a) Czerney P, Grummt U-W. *J. Chem. Res. (S)*, 1996; 173; (b) Czerney P, Grummt U-W. *J. Chem. Res. (M)*, 1996; 1001–1022.
4. Wirz J. *Pure Appl. Chem.* 1998; **70**: 2221–2232.
5. Katritzki AR, Czerney P, Levell JR, Du W. *Eur. J. Org. Chem.* 1998; 2623–2629.
6. Katritzki AR, Czerney P, J. R. Levell JR. *J. Org. Chem.* 1997; **62**: 8198–8200.
7. Rabinowitsch WA, Chawin EJ. *Kratkii Khimitscheskii Sprawotschnik*. Khimiya: Leningrad, 1978; 249.
8. Malinowski ER. *Factor Analysis in Chemistry* (2nd edn). Wiley: New York 1991; 32–82.
9. Schuetz H, Stutter E, Weller K, Petri I. *Stud. Biophys.* 1983; **10**: 23–34.
10. Frisch MJ, Trucks GW, Schlegel HB, Scuseria GE, Robb MA, Cheeseman JR, Zakrzewski VG, Montgomery JA Jr, Stratmann RE, Burant JC, Dapprich S, Millam JM, Daniels AD, Kudin KN, Strain MC, Farkas O, Tomasi J, Barone V, Cossi M, Cammi R, Mennucci B, Pomelli C, Adamo C, Clifford S, Ochterski J, Petersson GA, Ayala PY, Cui Q, Morokuma K, Malick DK, Rabuck AD, Raghavachari K, Foresman JB, Cioslowski J, Ortiz JV, Baboul AG, Stefanov BB, Liu G, Liashenko A, Piskorz P, Komaromi I, Gomperts R, Martin RK, Fox DJ, Keith T, Al-Laham MA, Peng CY, Nanayakkara A, Gonzalez C, Challacombe M, Gill PMW, Johnson B, Chen W, Wong MW, Andres JL, Gonzalez C, Head-Gordon M, Replogle ES, Pople JA. Gaussian 98, Revision A. 7. Gaussian: Pittsburgh, PA, 1998.
11. Onsager L. *J. Am. Chem. Soc.* 1936; **58**: 1486–1493.
12. Jurd L. *Tetrahedron* 1969; **25**: 2367–2380.
13. Matsushima R, Suzuki M. *Bull. Chem. Soc. Jpn.* 1992; **65**: 39–45.
14. Lietz H, Haucke G, Czerney P, John B. *J. Prakt. Chem.* 1996; **338**: 725–730.
15. (a) Grummt U-W. *J. Photochem.* 1983; **23**: 17–26; (b) Szabo ZG. In *Comprehensive Chemical Kinetics*, vol. 2, Bamford CH, Tipper DF (eds). Elsevier: Amsterdam, 1969; 342.
16. Jesser V. PhD Thesis, University of Jena, 1999.